UHV high-resolution electron microscopy and chemical analysis of room-temperature Au deposition on Si(001)-2×1

E. Landree,* D. Grozea, C. Collazo-Davila, and L. D. Marks
Department of Materials Science and Engineering, Northwestern University, Evanston, Illinois 60208
(Received 31 July 1996)

Investigations of Au on Si(001) have suggested that room-temperature deposition of Au on a clean Si surface results in an interfacial reaction and the formation of a gold-silicide. However, these investigations typically lack direct information about the surface morphology or the exact structure at the interface. Utilizing the capabilities of a surface chemical analysis system attached to a Hitachi UHV H-9000 microscope, a layer plus island growth mode has been observed by high-resolution electron microscopy showing multiply twinned small particles on the surface. The presence of small particles for various coverages has been correlated with the shifts seen in the Si $2p$ and Au $4f$ binding energies as well as the peak splitting in the Si LVV Auger transition. Our chemical data are consistent with observed shifts in the binding energies of small metal clusters deposited on various substrates, and with the published data for this surface. In addition, the results are consistent with our previous studies of Ag on Si(001), and indicate the growth morphology plays a crucial role in understanding spectroscopic information as well as its correlation to the structure and chemical state of the interface and surface morphology. [S0163-1829(97)08111-3]

I. INTRODUCTION

Starting in the early 1970s, the gold-silicon interface has been extensively investigated using various surface techniques to better understand its crystallographic, chemical, and electronic properties. Despite the Au/Si contact being unsuitable for applications in integrated circuit devices due to the rapid diffusion of Au atoms and their deep-trap center formation in Si, the study of thin Au films on Si still raises interesting questions. Areas of interest include the supposed Au-Si reaction at room temperature (RT) and the critical gold coverage necessary to induce it, the diffusion of Si through Au layers even for thick deposits, and related properties such as the origin and structure of electronic states at the interface.

In spite of the many different surface techniques which have been used to study thin Au films on Si at RT, due to the difficulty of obtaining a direct correlation between electronic and morphological properties of the system there is little agreement over the exact nature of the interface. A nonexhaustive list of the techniques used, individually or combined, includes low-energy electron diffraction (LEED),[1–9] Auger electron spectroscopy (AES),[2–4,6–8,10–13] MeV ion backscattering,[14–17] electron-energy-loss spectroscopy (EELS),[4,6,8–20] x-ray photoelectron spectroscopy (XPS),[21] ultraviolet photoelectron spectroscopy (UPS),[20,22–25] photoemission yield spectroscopy,[7] soft-x-ray photoelectron spectroscopy,[26] scanning tunneling microscopy (STM),[27] x-ray standing wave,[28] and transmission electron microscopy (TEM).[6,8,29]

The contradictory results which have been reported may be due to different experimental conditions such as unknown defect concentration on the reconstructed silicon surface, the estimation of the Au thickness, assumptions concerning the growth morphology, and neglect of the Au cluster size effect on the electronic properties and spectroscopic data.

The structure of the interface, whether it is abrupt or diffuse, and the subsequent issue of a stable, nonreactive metal interacting with the silicon surface at room temperature, is an issue of debate. Several models have tried to explain how the Si bond breaking occurs, and how a Au-Si compound, intermixed phase, alloy or silicidelike material is formed. The proposed models include the ''glassy membrane model,''[30] the ''interstitial model,''[12,19,22,31] the ''electrostatic screening model,''[32] and the ''chemical bonding model'' based on charge transfer.[24]

LEED studies have reported a gradual fading of the surface spots into a high diffuse background with increasing Au coverage. To our knowledge only one paper identifies a weak, diffuse ring whose spacing was attributable to neither Si nor Au (Ref. 3) at 30 Å of Au on Si(001). LEED was typically used in conjunction with AES, which used the Si LVV 92-eV peak splitting, reported to occur at a coverage of one to several monolayers of Au,[4,12,18] to constitute ''proof'' of a silicide.[11,14,21] This explanation of the Si LVV line-shape modification is still a matter of controversy.[12,33]

UPS and EELS studies supported the formation of a silicide at various Au coverages at the interface or only as a surface thin layer on top of the Au deposit.[4,18,19,22,24] However, the building of the Fermi energy step at ~0.33 ML of Au, attributed to early alloy formation, can be due to gold clustering.[23] Recent high-resolution EELS and UPS experiments also indicate the presence of pure Au clusters in the first few Au-Si layers,[20] in opposition to STM results[27] which reported a layer-by-layer growth.

In the present paper, we report the investigation of initial growth of Au on the Si(001)-2×1 surface at RT using a system combining high-resolution electron microscopy with several surface techniques, e.g., AES, XPS, and scanning electron microscopy, while maintaining ultrahigh-vacuum (UHV) conditions.

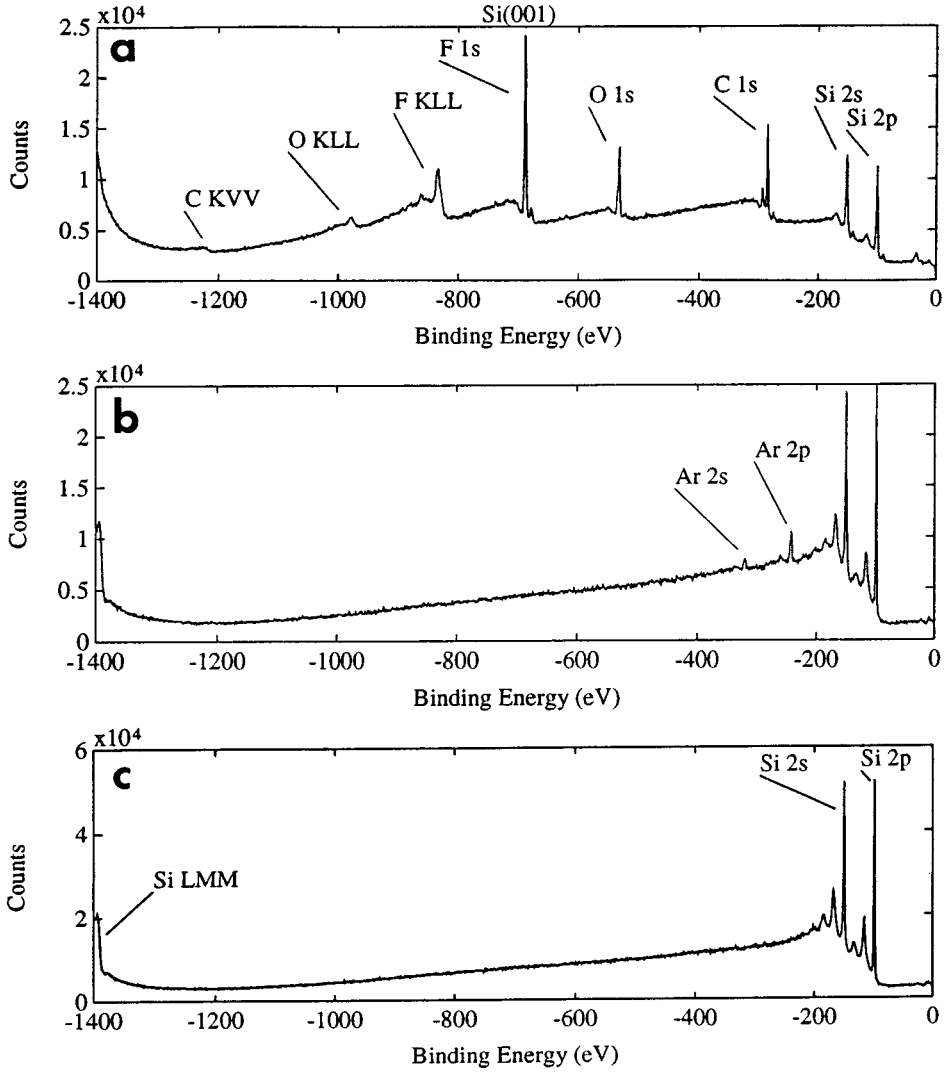

FIG. 1. XPS spectrum of an (a) as-etched Si(001) surface, (b) after argon milling, and (c) after annealing.

II. EXPERIMENTAL PROCEDURE

Ex situ sample preparation consisted of cutting 3-mm disks from *p*-type Si(001) wafers of 13.5–18.5 Ω cm. The specimen surface was then dimpled and polished to roughly 20 μm at the center. Afterwards it was chemically etched in a solution of 10% HF, 90% NHO_3 until the sample became perforated. After transferring it to a molybdenum sample holder, it was introduced into the surface preparation and analysis system (SPEAR).[34] SPEAR is a multichamber ultrahigh-vacuum surface characterization and preparation system which is attached to a Hitachi UHV H-9000 high-resolution transmission electron microscope.[35,36] This design allows for samples to be transferred between the microscope and SPEAR while preserving UHV conditions at all times.

Samples were prepared *in situ* through iterative cycles of oxygen and argon-ion milling and direct electron-beam annealing. The chemical state of the surface was characterized using XPS and AES. Figure 1 is an example of an as etched Si(001) sample surface after introduction into the system and the sample surface following several cycles of milling and annealing. Once contamination levels were at or near the detection limit of the instruments, the sample was transferred into the microscope for surface structure characterization.

The surface was characterized using surface-sensitive techniques such as XPS, AES, and off-zone transmission electron diffraction (TED). Samples needed to be sufficiently thin for high-resolution electron microscopy and have low surface defect density, monitored using dark-field (DF) transmission electron microscopy, to avoid possible influence on the film growth mode.[37,38]

Figure 2 is an off-zone high-resolution electron micrograph taken at 200 kV of a clean Si(001)-2×1 surface prior to Au deposition. The diagonal lines of contrast correspond to the Si(001) surface dimers along the $\langle 110\rangle$ directions and are spaced 7.68 Å apart. This spacing is two times the surface unit mesh. The boundary line separating the 1×2 and 2×1 domains across the center of the image corresponds to a single atomic step on the surface.

It was determined that the electron-beam annealing produced a disordered surface on the incident side of the sample to the electron beam, and well-ordered steps on the exit surface.[39] Consequently, all Au depositions in this study were performed only on the ordered surface.

Au was deposited with the sample at RT using a tungsten thermal evaporation stage located in the transfer module of SPEAR. The tungsten boats were carefully outgassed prior to

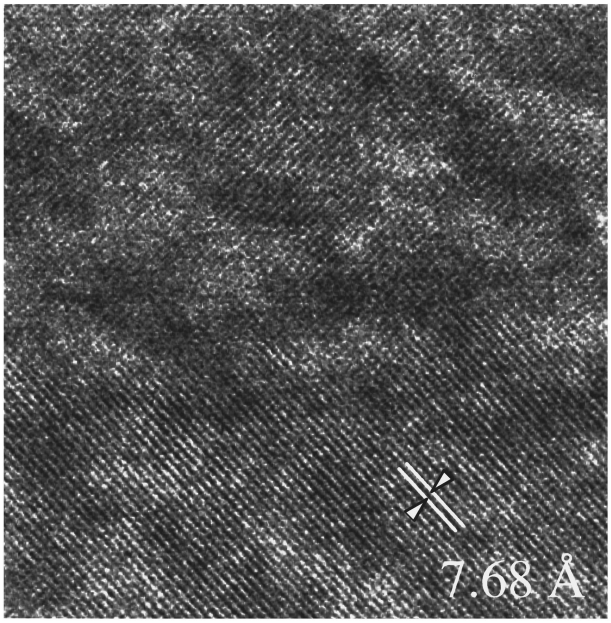

FIG. 2. Off-zone high-resolution image of Si(001)-2×1 surface taken at 200 kV. 7.68 Å is two times the 1×1 surface unit mesh and corresponds to the spacing between the Si dimer rows.

deposition. Au coverages were estimated using the relative Si $2p$ and Au $4f$ XPS peak intensities collected over an 800-μm-diameter area. After each deposition XPS and AES were performed, and transmission electron diffraction and high resolution electron microscopy images were recorded at 300 kV.

III. RESULTS

At low coverages a diffuse ring appears coincident with the Au(111) spacing. Figure 3 is a diffraction pattern taken after roughly 2 Å of Au deposition. Diffuse spots along the ring indicate that oriented growth is present at the initial stage of deposition. Figure 4 is an image of the surface at the same coverage.

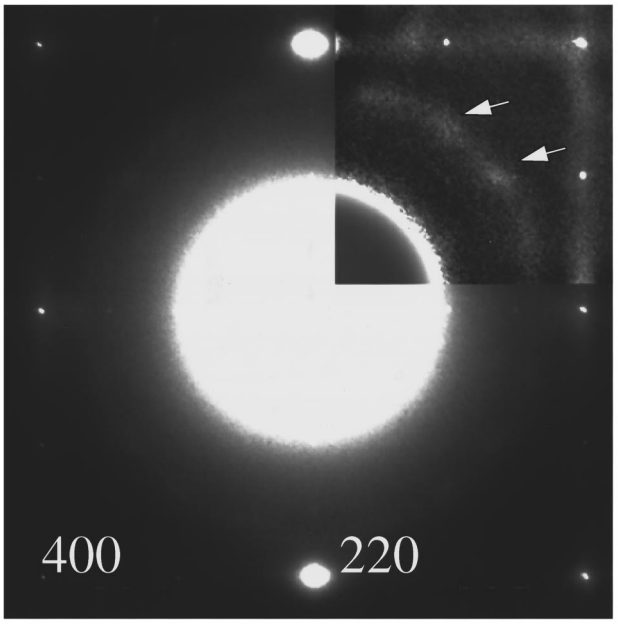

FIG. 3. TED pattern of the Si(001) surface following 2 Å of Au deposition.

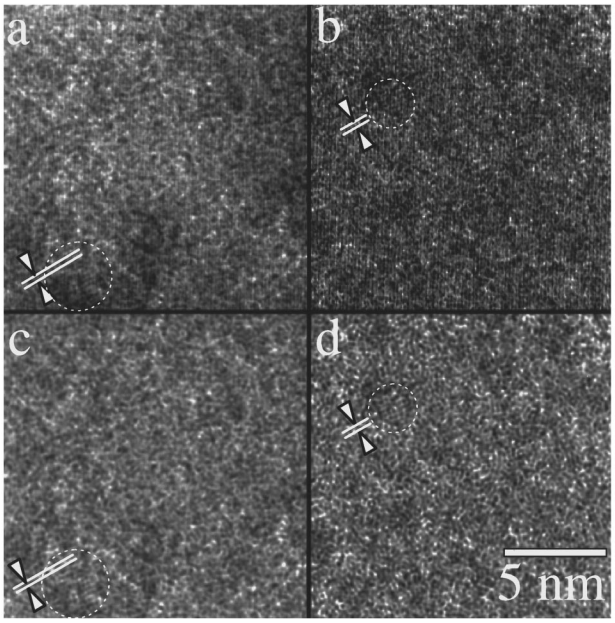

FIG. 4. High-resolution image of the Si(001) surface following 2 Å of Au deposition. (a) and (b) are unfiltered images of surface regions showing oriented growth. Fringes coincident with the Au(111) spacing have been arrowed for reference. (c) and (d) show the same region after Fourier filtering to remove spacings smaller than 2.34 Å.

Steps observed on the Si(001)-2×1 surface using DF transmission electron microscopy prior to deposition disappear as Au is deposited. Figure 5 is a DF image taken at 200 kV from the same region of the sample before and after 8 Å Au deposition. The steps disappearance can be attributed to a disordering of the Si surface induced by the presence of Au.

At higher coverages, TEM micrographs show the presence of multiply twinned and single-crystal small particles nucleating on the surface, Fig. 6. This is similar to observations of RT growth and nucleation of Ag on Si(001)-2×1.[40] Figure 7(a) is an off-zone TED pattern of the sample at the same coverage and Fig. 7(b) is a schematic representation. The rings are coincident with the Au(111) and Au(200) spacings. The bright spots along the rings indicate a Au(110)//Si(001) epitaxy on the two Si(001)-2×1 domains, 2×1 and 1×2, which are rotated by 90°. At no point did there appear any unidentifiable features to support the formation of a structured gold-silicide.

Figure 8 is a TED pattern taken at a longer exposure time from the same region as Fig. 7(a). Intensity along the entire Au rings indicates the presence of small domain polycrystalline gold. Another notable feature is the presence of Si(001)-2×1 spots at 13 Å of Au. This is contradictory to results from previous LEED studies, which conclude that the 2×1 superstructure and 1×1 spots disappear for lower gold coverages.[3,5,7,8,25] More than 172 h after the initial deposition, superstructure spots with a 2×1 periodicity were still evident in the TED pattern, Fig. 9. XPS measurements detected chemisorbed oxygen on both sides of the sample. There was also no gold detected on the native, undeposited

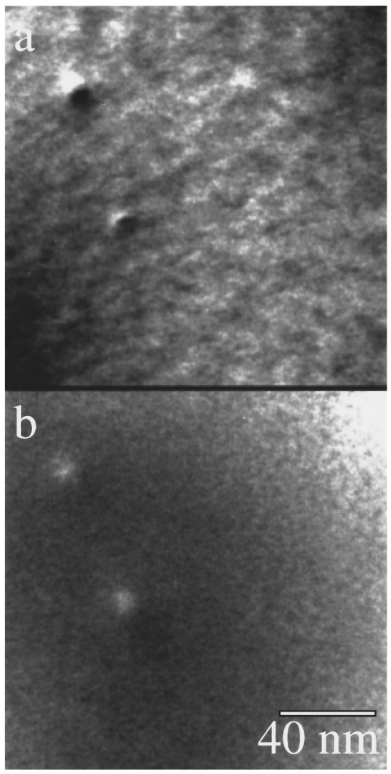

FIG. 5. Dark-field image of the Si(001) surface taken at 200 kV using the Si(220) reflection (a) prior to deposition, showing well-ordered surface steps. (b) After 8 Å of Au deposition, surface steps are no longer present.

silicon surface. The destructive effect of water vapor on the Si(001)-2×1 reconstruction[41] and the presence of oxygen indicates the observed 2×1 periodicity must exist at the interface between the Au overlayer and the Si substrate, suggesting that a 2×1 structure is preserved underneath the gold overlayer on the Au-deposited side of the sample.[42]

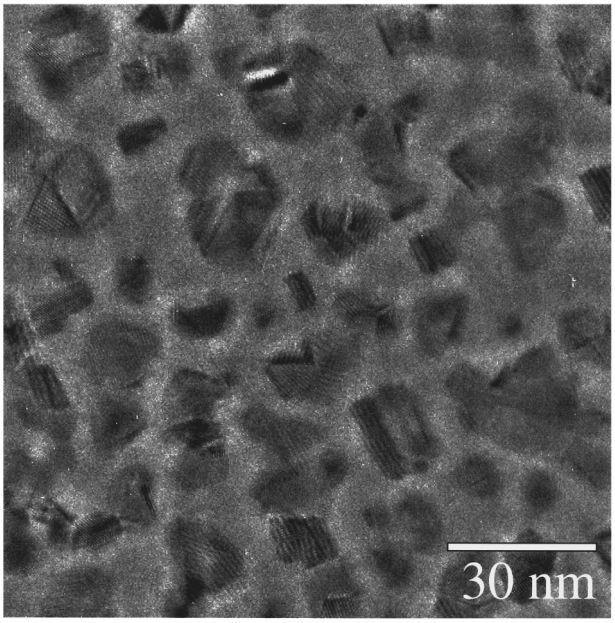

FIG. 6. High-resolution image of the Si(001) surface following 13 Å of Au deposition.

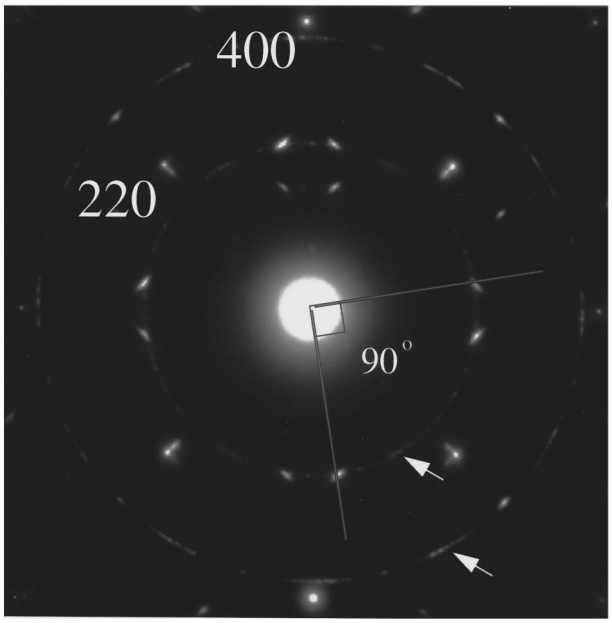

(a)

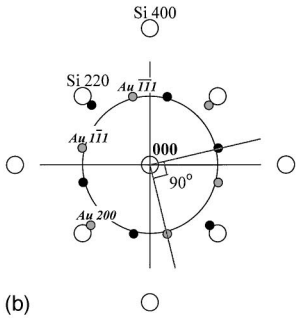

(b)

FIG. 7. (a) TED pattern of the Si(001) surface after 13 Å of Au deposition showing the Au(110)//Si(001) epitaxy on the two Si(001)-2×1 domains. Amorphous rings coincident with the Au(111) and Au(220) spacings have been arrowed for reference. (b) Schematic representation of Fig. 7(a). The two different surface domains are separated by a 90° rotation, which has been labeled for reference.

Shifts in the binding energies of the Au $4f$ and Si $2p$ peaks have been observed during Au deposition. Figure 10 is a plot of the shifts in the relative binding energies of the Au $4f_{7/2}$ and Si $2p$ peaks as a function of gold coverage. Results show a sudden increase in the Au $4f$ binding energy with the first few Å of Au deposition. With additional deposition, beyond roughly 2 Å, the binding energy gradually decreases, tending toward bulk values as the coverage increases. The Si $2p$ peak illustrates the opposite trend, showing a shift to lower binding energies followed by a return to the bulk Si binding energy as the Au coverage is increased. Our results are consistent with previous studies, which suggested the peak shifts indicate an interaction at the Au-Si interface and the presence of a chemical reaction owing to the formation of a gold-silicide.[21,22] These results are also consistent with the recent studies by Vijayakrishnan and Rao, which showed that a similar trend is also found in metal deposition studies on various substrates.[43,44]

AES spectra acquired at different stages of deposition

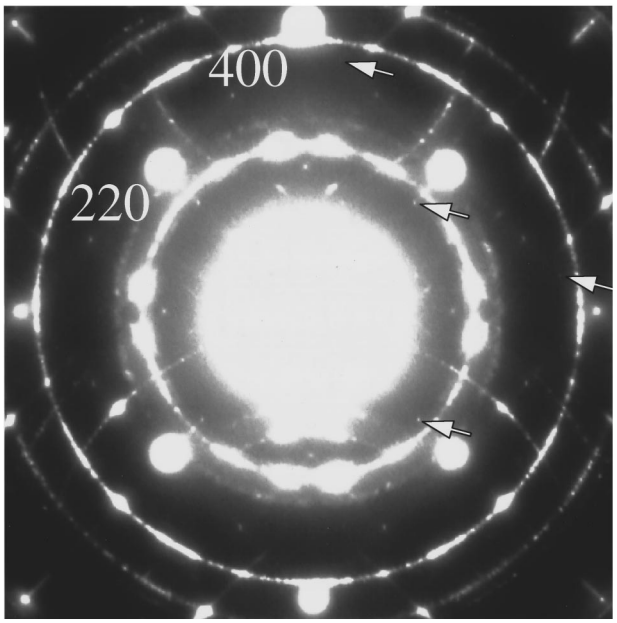

FIG. 8. A longer exposure time TED pattern of the Si(001) surface following 13 Å of Au deposition. The Si(001)-2×1 surface superstructure spots have been arrowed for reference.

show the characteristic appearance of a split in the Si *LVV* Auger transition which has been used to indicate the formation of a gold-silicide. Figure 11 is a montage of AES spectra taken at different stages of deposition. The corresponding TED pattern and high-resolution electron microscopy image for a Au coverage of 13 Å, Figs. 4 and 5, show no evidence of a structured gold silicide which could contribute to the splitting in the AES spectrum. This indicates an upper limit of less than 0.1 ML of silicide; more than this amount would have been detectable by transmission electron microscopy techniques.

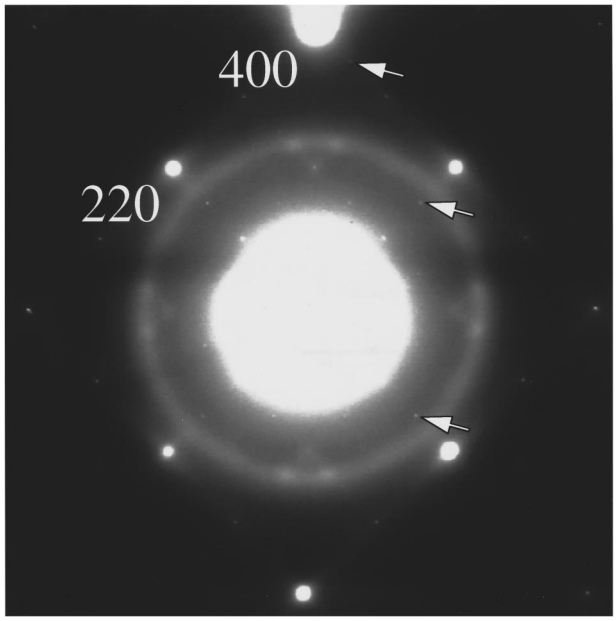

FIG. 9. A TED pattern of the Si(001) surface following 8 Å of Au deposition after storing under 1×10^{-10} Torr for 172 h. Si(001)-2×1 spots are still present and have been arrowed for reference.

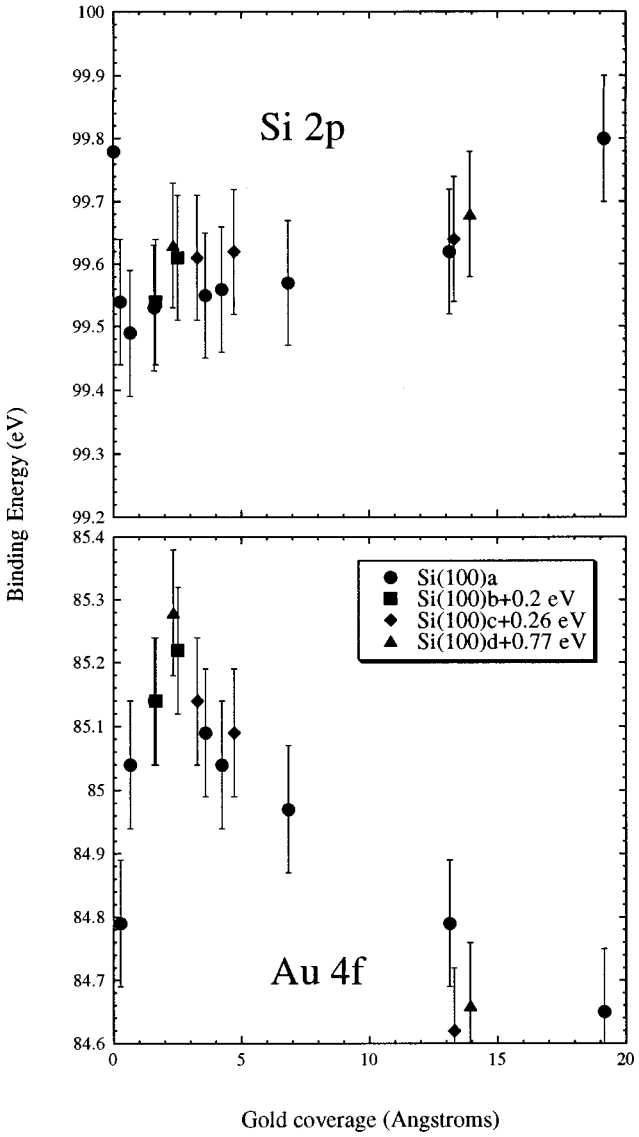

FIG. 10. Shifts in the Si $2p$ and Au $4f_{7/2}$ peak as a function of Au coverage. Si(001)a–d are four different samples studied including the relative calibration offset. These offset values were measured using XPS by scanning over the Si $2p$ peak for each sample prior to Au deposition, and then adjusting relative to the Si $2p$ bulk value.

The Au Auger line also appears to shift to higher kinetic energies with increasing gold particle size on the surface and is consistent with a study by Oberli *et al.*,[45] which examines the AES spectra for small gold particles on amorphous carbon.

IV. DISCUSSION

All of our spectroscopic chemical data are consistent with earlier results presented in the literature. However, the growth mode for the system is not what was previously assumed.[4,12,27] From microscopy images and electron-diffraction information, we have directly observed evidence of Stranski-Krastanov growth mode, layer plus island (or at least pseudo-Stranski-Krastanov growth, incomplete first layer plus islands), not layer by layer. At low coverages, a

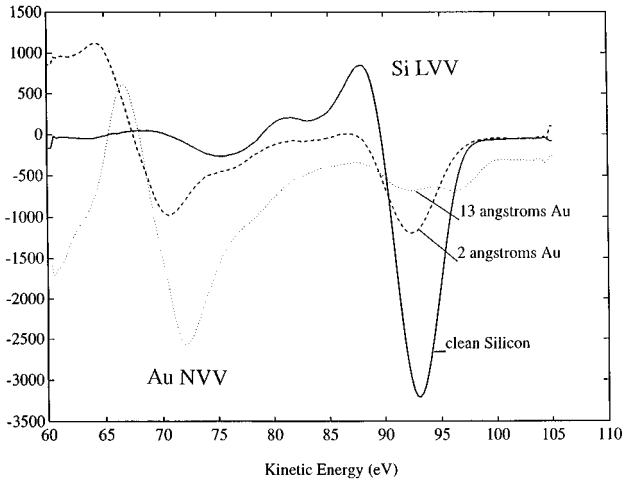

FIG. 11. Line shape of the Si *LVV* and Au *NVV* Auger transitions as a function of Au coverage. Each spectrum has an uncertainty of $\sigma = 0.8$ eV.

diffuse ring coincident with the Au(111) spacing in the diffraction pattern indicates the existence of an amorphous glassy layer. Diffuse spots along the ring verify the presence of islands from the early stages of deposition. Multiply twinned and single-crystal small particles are evident from micrographs of the surface at 13-Å gold coverage.

The disappearance of the surface steps from the initial stages of deposition suggests that Au disorders the surface, and a disordered two-dimensional Si-Au glassy layer is formed. This is also supported by a mottled background present throughout the high-resolution transmission electron microscopy images, Fig. 4. This is consistent with previous studies which have observed the formation of this glassy layer,[46,47] and can be attributed to the high entropy of mixing in the Au-Si system.[33] The sudden shifts in the Au and Si binding energies at the early stages of deposition, up to roughly 2 Å, also coincide with the formation of the Au-Si glassy phase on the surface.

Results from Vijayakrishnan and Rao[43,44] showed that the size of small metal clusters on various substrates influenced the relative binding energy of the metal. Their model suggested that this is due to the inability of small particles to shield the core hole created during photoemission. They argued that this results in an increasing relative binding energy with decreasing particle size. Conversely, the core hole created is well screened in bulk metals and large particles. Therefore, increasing particle size or increasing coverage results in a decreasing relative binding energy. Regardless of the validity of this model, we can attribute the shifts seen in the Au on Si XPS spectroscopic data to the growth of small particles.

From the images and diffraction data, the silicon atoms at the surface appear to sit in two different environments. In one environment the silicon atoms sit below the particles. In the other the atoms are underneath an amorphous or disordered layer that exists between the particles. It is therefore reasonable that the silicon in these different environments contributes to the peak splitting of the Si *LVV* transition observed in the Auger spectrum. While at this point we cannot comment on the presence of a structured silicide which may exist in quantities substantially less than a monolayer, or an amorphous silicide which may exist on the order of a couple of monolayers after room temperature deposition, we do see disordering of the surface steps induced by the presence of Au on the surface to suggest a two-dimensional glassy layer. However, electron microscopy images and transmission electron diffraction information show there is insufficient silicide present to explain the recorded shifts in the XPS spectra and the Si peak splitting observed in the AES spectra.

Studies of bulk Au and Si mixtures, as well as thick films of Au on Si, have produced metastable gold silicide phases.[48–51] Similarly, studies of gold thin films on silicon have also reported evidence of silicides after annealing at or above the Au-Si eutectic temperature.[1,3,52–54] There is, however, no structural evidence of the presence of a gold silicide following room temperature deposition.

This study illustrates the difficulty in using spectroscopic data alone to indicate the presence of a change in chemical state conclusively, since it has been shown that the surface growth morphology can influence relative shifts in the XPS and AES spectra.

ACKNOWLEDGMENTS

We would like to acknowledge the support of the National Science Foundation on Grant No. DMR-9214505 and the support of the Air Force Office of Scientific Research on Grant No. F49620-94-1-0164 in funding this work.

*Electronic address: e-landree@nwu.edu

[1] A. K. Green and E. Bauer, J. Appl. Phys. **47**, 1284 (1976).
[2] K. Oura, Y. Makino, and T. Hanawa, Jpn. J. Appl. Phys. **15**, 737 (1976).
[3] K. Oura and T. Hanawa, Surf. Sci. **82**, 202 (1979).
[4] K. Okuno, T. Ito, M. Iwami, and A. Hiraki, Solid State Commun. **34**, 493 (1980).
[5] A. K. Green and E. Bauer, Surf. Sci. **103**, L127 (1981).
[6] G. Le Lay, J. Cryst. Growth **54**, 551 (1981).
[7] A. Taleb-Ibrahimi, C. A. Sebenne, D. Bolmont, and P. Chen, Surf. Sci. **146**, 229 (1984).
[8] M. Hanbucken, Z. Imam, J. J. Metois, and G. Le Lay, Surf. Sci. **162**, 628 (1985).
[9] K. Meinel and D. Katzer, Appl. Surf. Sci. **56-58**, 514 (1992).
[10] M. T. Thomas and D. L. Styris, Phys. Status Solidi B **57**, K83 (1973).
[11] T. Narusawa, S. Komiya, and A. Hiraki, Appl. Phys. Lett. **22**, 389 (1973).
[12] H. Dallaporta and A. Cros, Surf. Sci. **178**, 64 (1986).
[13] V. K. Adamchuk and A. M. Shikin, J. Electron Spectrosc. Relat. Phenom. **52**, 103 (1990).
[14] K. Nakashima, M. Iwami, and A. Hiraki, Thin Solid Films **25**, 423 (1975).
[15] T. Narusawa, K. Kinoshita, and W. M. Gibson, J. Vac. Sci. Technol. **18**, 872 (1981).
[16] T. Narusawa, W. M. Gibson, and A. Hiraki, Phys. Rev. B **24**, 4835 (1981).
[17] H. S. Jin, T. Ito, and W. M. Gibson, J. Vac. Sci. Technol. A **3**, 942 (1985).

[18] P. Perfetti, S. Nannarone, F. Patella, C. Quaresima, A. Savoia, F. Cerrina, and M. Capozi, Solid State Commun. **35**, 151 (1980).
[19] F. Salvan, A. Cros, and J. Derrien, J. Phys. Lett. **41**, L337 (1980).
[20] G. Mathieu, R. Contini, J. M. Layet, P. Mathiez, and S. Giorgio, J. Vac. Sci. Technol. A **6**, 2904 (1988).
[21] A. Hiraki and M. Iwami, Jpn. J. Appl. Phys. Suppl. **2**, 749 (1974).
[22] L. Braicovich, C. M. Garner, P. R. Skeath, C. Y. Su, P. W. Chye, I. Lindau, and W. E. Spicer, Phys. Rev. B **20**, 5131 (1979).
[23] K. Hricovini, J. E. Bonnet, B. Carriere, J. P. Deville, M. Hanbucken, and G. Le Lay, Surf. Sci. **211/212**, 630 (1989).
[24] M. Iwami, T. Terada, H. Tochihara, M. Kubota, and Y. Murata, Surf. Sci. **194**, 115 (1988).
[25] Z. H. Lu, T. K. Sham, K. Griffiths, and P. R. Norton, Solid State Commun. **76**, 113 (1990).
[26] L. J. Brillson, A. D. Katnani, M. Kelly, and G. Margaritondo, J. Vac. Sci. Technol. A **2**, 551 (1984).
[27] X. F. Lin and J. Nogami, J. Vac. Sci. Technol. B **12**, 2090 (1994).
[28] S. M. Durbin, L. E. Berman, B. W. Batterman, and J. M. Blakely, Phys. Rev. B **33**, 4402 (1986).
[29] C. R. Chen and L. J. Chen, J. Appl. Phys. **78**, 919 (1995).
[30] R. W. Walser and R. W. Bene, Appl. Phys. Lett. **28**, 624 (1976).
[31] K. N. Tu, Appl. Phys. Lett. **27**, 221 (1975).
[32] A. Hiraki, Surf. Sci. Rep. **3**, 357 (1984).
[33] S. Cros and P. Muret, Mater. Sci. Rep. **8**, 271 (1992).
[34] C. Collazo-Davila, E. Landree, D. Grozea, G. Jayaram, R. Plass, P. Stair, and L. D. Marks, J. Microsc. Soc. Am. **1**, 267 (1995).
[35] J. Bonevich and L. D. Marks, Microscopy **22**, 95 (1992).
[36] G. Jayaram, R. Plass, and L. D. Marks, Interf. Sci. **2**, 379 (1995).
[37] J. A. Venables, G. D. T. Spiller, and M. Hanbucken, Rep. Prog. Phys. **47**, 399 (1984).
[38] M. Henzler, Surf. Sci. **357-358**, 809 (1996).
[39] E. Landree, D. Grozea, and L. D. Marks (unpublished).
[40] N. Doraiswamy, G. Jayaram, and L. D. Marks, Phys. Rev. B **51**, 10 167 (1995).
[41] Y. Boland, Phys. Rev. Lett. **65**, 3325 (1990).
[42] A. Stierle, T. Muhge, and H. Zabel, J. Mater. Res. **9**, 884 (1994).
[43] V. Vijayakrishnan and C. N. R. Rao, Surf. Sci. Lett. **255**, L516 (1991).
[44] C. N. R. Rao, Solid State Ionics **63-65**, 835 (1993).
[45] L. Oberli, R. Monot, H. J. Mathieu, D. Landolt, and J. Buttet, Surf. Sci. **106**, 301 (1981).
[46] A. Hiraki, A. Shimizu, M. Iwami, T. Narusawa, and S. Komiya, Appl. Phys. Lett. **26**, 57 (1975).
[47] W. Robison, R. Sharama, and L. Eyring, Acta Metall. Mater. **39**, 179 (1991).
[48] G. A. Andersen, J. L. Bestel, A. A. Johnson, and B. Post, Mater. Sci. Eng. **7**, 83 (1971).
[49] H. L. Gaigher and N. G. Van Der Berg, Thin Solid Films **68**, 373 (1980).
[50] N. G. Dhere and C. de A. Loural, Thin Solid Films **81**, 213 (1981).
[51] H. Kato, Jpn. J. Appl. Phys. **28**, 953 (1989).
[52] Z. H. Lu, T. K. Sham, and P. R. Norton, Solid State Commun. **85**, 957 (1993).
[53] X. F. Lin, K. J. Wan, J. C. Glueckstein, and J. Nogami, Phys. Rev. B **47**, 3671 (1993).
[54] G. Jayaram and L. D. Marks, Surf. Rev. Lett. **2**, 731 (1995).